Inversion Algorithms for Particle Sizing with Photon Migration Measurement

Zhigang Sun
Dept. of Chemical Engineering, Texas A&M University, College Station, TX 77843
and
School of Chemical Engineering, Purdue University, West Lafayette, IN 47907

Eva M. Sevick-Muraca
Dept. of Chemical Engineering, Texas A&M University, College Station, TX 77843

A new linear inverse method is demonstrated for recovery of particle-size distribution (PSD) and volume fraction of opaque colloidal suspensions from frequency domain photon migration (FDPM) measurement of multiply scattered light. To deal with the ill posedness of PSD retrieving problem, the size distribution is approximated by the B-spline expansion. Tikhonov regularization, along with both nonnegativity and smoothing constraints, in which the L-curve method is employed to choose a regularization parameter, are also used to ensure the stable and realistic solution. The algorithm is tested using synthetic FDPM measurements at a variety of size distributions, and results are compared using other inverse methods. The influences of model and measurement error are investigated. To demonstrate our inversion approach, PSD and volume fraction of opaque titanium dioxide suspensions are recovered from actual FDPM measurements. This work demonstrates the ability of FDPM method to characterize colloidal suspensions.

Introduction

Online measurements of particle-size distribution (PSD) and volume fraction of colloidal suspensions are highly desired in the particulate processes of pharmaceutical and chemical industries in order to effectively evaluate, optimize, and control manufacturing processes and product quality. However, it is difficult to obtain these critical parameters at industrially relevant concentrations using real-time, online measurements. Most available online particle sizing methods, such as turbidity (Crawley et al., 1997), angular static scattering (Frock, 1987), and dynamic light scattering (Nicoli et al., 1991), are based on single light scattering principle. Each method requires considerable sample dilution and measurement calibration due to the confounding effects of multiple scattering from concentrated suspensions. Although some modifications of above methods, such as fiber optic dynamic light scattering (FODLS) (Thomas, 1991) and modified static light scattering (SLS) (Lehner et al., 1998), have been proposed to suppress the effects of multiple scattering, these methods are not well suited for particle sizing on multiple scattering, concentrated colloidal suspensions.

In recent years, new particle-sizing methods based on multiple light scattering principle, such as diffusive wave spectroscopy (DWS) (Horne and Davidson, 1993) and acoustic spectroscopy (AS) (Alba et al., 1999), have been applied for particle sizing in concentrated suspensions. Frequency domain photon migration (FDPM) is yet another new potential method for online characterization of multiple scattering, concentrated colloidal suspensions (Sevick-Muraca et al., 1997). Since this technique measures time-dependent propagation characteristics rather than the amount of light detected, it is self-calibrating and no external calibration is required. In addition, FDPM allows independent determination of absorption and scattering. Consequently, characterization of colloidal scatters is not biased by changes in the light absorption or color of suspending fluids. Because FDPM depends upon multiple scattered light, it is restricted to nondilute particulate suspensions, whereby the suspensions are typically opaque. Both size distribution and volume fraction can be directly obtained by inversion algorithms, where

Correspondence concerning this article should be addressed to E. M. Sevick-Muraca.

the only physical parameter required is the relative refractive index between the particulate and continuous phases. Since no dilution is necessary to avoid multiple scattering, FDPM is suitable for online monitoring PSD and volume fraction in particulate processes.

Recently, we have demonstrated that FDPM can be successfully used for recovery of PSD and volume fraction in opaque, multiple scattering suspensions of polystyrene and titanium dioxide (Sevick-Muraca et al., 1997; Richter et al., 1998). Using visible wavelengths, particles from 50 nm to 1 micron may be characterized at multiple scattering, noninteracting suspensions. However, at high volume fractions (such as larger than 5%), corrections for particle interaction are necessary (Shinde et al., 1999; Richter and Sevick-Muraca, 2000). To date, our work on FDPM has been limited by the requirement to make *a priori* assumptions of the PSD, whether described by normal, log-normal, or Weibull distributions. The parameters, which describe the distributions, are determined by a best-fit procedure on the experimental data using nonlinear least-squares regression. In this contribution, we seek to recover the volume fraction and the PSD of arbitrary form without *a priori* information.

Recovery of PSD from light scattering measurements involves solving a set of Fredholm integral equations of the first kind. As a well-known ill-posed problem, it is characterized by incompleteness of available information, nonuniqueness of its solution, and noncontinuous dependence of the solution on the available data. Moreover, the solution is extremely sensitive to small perturbations of the system (that is, measurement error) so that all classical numerical methods fail to obtain a meaningful solution. Aimed at the difficulties of solving general Fredholm integral equations, several inversion algorithms have been proposed and used in a variety of applications. These methods include: Tikhonov regularization (Tikhonov and Arsenin, 1977); least squares with physical constraints (Copper and Spielman, 1976; Amato et al., 1996); truncated single value decomposition (SVD) and generalized SVD (GSVD) (Hansen, 1990; Xu, 1998); Chahine's (1968) and Twomey's (1975) nonlinear iterative methods with modifications (Ferri et al., 1995; Markowski, 1987); Landweber and accelerated Landweber iterative regularization methods (Carfora et al., 1998); extreme value estimation (Aalto et al., 1990; Hopke and Paatero, 1994); and maximum entropy (Amato and Hughes, 1991). These methods attempt to transform the ill-posed problem into a nearby well-posed problem by introducing additional constraints on the solution. In recent years, other methods have been proposed for solving the ill-posed problem of particle sizing, such as neural network (Nascimento et al., 1997), Bayesian analysis (Ramachandran and Kandlikar, 1996a), inverse Monte Carlo (IMC) (Ligon et al., 1996), genetic algorithm (GA) (Ye et al., 1999), and wavelet-based regularization methods (Frontini and Chaubell, 1999). However, few have been tested with real experimental data.

The majority of these algorithms are used in aerosol science and geophysics, with only a few attempted for recovering free-form PSD from scattering measurements in colloidal suspensions. In this work, we develop a linear inverse method for recovery of free-form size distribution and volume fraction from FDPM measurements of opaque colloidal suspensions. We employ three strategies to obtain a stable and physically reasonable solution of the ill-posed inverse problem: (1) B-spline approximation of an unknown function; (2) Tikhonov regularization along with both non-negativity and smoothing constraints; and (3) L-curve method used for selecting the regularization parameter. The advantages of our approach are: (1) the requirement to assume the form of the size distribution *a priori* can be avoided; (2) the recovery of multi-modal size distributions is possible; (3) the linear inversion is fast and suitable for determination of online PSD and volume fraction in industries.

In the following sections, we briefly introduce the FDPM measurement and theory for completeness, and formulate the free form PSD inversion problem before providing details of our new linear inverse method. We demonstrate this algorithm by recovering a variety of size distributions (that is, unimodal and bimodal, normal and log-normal, narrow and broad) using synthetic FDPM measurements and comparing them with other inverse approaches. The impact of model and measurement errors upon PSD recovery is also investigated. Finally, as a practical application, our inverse method is used for recovery of PSD and volume fraction of opaque titanium dioxide suspensions using actual FDPM measurements.

Background: Frequency Domain Photon Migration Measurement

In contrast to the DWS and AS methods, the FDPM method monitors the time-dependent propagation characteristics of multiply scattered light. This technique depends on launching intensity-modulated light into a multiple scattering medium at a single point source and detecting, at other points some distance away from the source, the amplitude attenuation and the phase shift of scattered light relative to the source light. Since the propagation of light in concentrated, multiple scattering particulate suspensions is modeled as a diffusion process, the measurement data can be regressed to obtain the optical properties of the colloidal suspension (that is, the absorption coefficient μ_a and the isotropic scattering coefficient μ_s') by solving the diffusion equation with appropriate boundary conditions (Duderstadt and Hamilton, 1976; Ishimaru, 1978; Fishkin et al., 1995). The wavelength-dependent isotropic scattering coefficients are associated with particle-size distribution and volume fraction by light scattering theory, which is the theoretical basis of photon migration technique for particle characterization.

If interparticle interactions are assumed to be negligible, the Mie theory can be used to describe the association between the isotropic scattering coefficient and particle size of suspensions. For polydisperse system, the isotropic scattering coefficient can be predicted by

$$\mu_s'(\lambda) = \int_0^\infty \frac{3}{2} \frac{Q_{\text{scat}}(x, \lambda)}{x} [1 - g(x, \lambda)] \phi f(x) dx \quad (1)$$

where x is the particle diameter; $f(x)$ is the particle-size distribution (PSD); ϕ is the particle volume fraction; λ is wavelength; $Q_{\text{scat}}(x, \lambda)$ is the angle-integrated scattering efficiency; and $g(x, \lambda)$ is the scattering anisotropy, which is the mean cosine of the scattering angle. Both scattering efficiency and scattering anisotropy can be predicted from scattering Mie theory (Bohren and Huffman, 1983). Alternately,

if particle concentrations are high and excluded volume and other particle interactions are involved, the formalism must be modified to include static structure (Richter and Sevick-Muraca, 2000). Nonetheless, upon measuring isotropic scattering coefficients at different wavelengths using FDPM, the inverse problem of determining $f(x)$ and ϕ requires solution of the Fredholm integral Eq. 1.

Equation 1 can be generalized as the following set of integral equations.

$$\mu_s'(\lambda_i) = \int_{a_1}^{a_2} K(x, \lambda_i) p(x) dx + e_i \qquad i = 1, 2, \ldots M \quad (2)$$

where $K(x, \lambda_i)$ is the kernel function, which is given by

$$K(x, \lambda_i) = \frac{3Q_{\text{scat}}(\lambda_i, x)}{2x}\left[1 - g(\lambda_i, x)\right] \qquad i = 1, \ldots, M \quad (3)$$

Here $\mu_s'(\lambda_i)$ is the discrete set of measurement data at M different wavelengths; $p(x)$ is the unknown function to be determined; a_1 and a_2 are the size limits within which the size distribution lies; and e_i is the measurement error.

Equations 2 and 3 constitute the inversion problem for recovering an unknown function $p(x)$ from discrete measurement data $\mu_s'(\lambda_i)$. In our method, the unknown function $p(x)$ is the product, $\phi f(x)$ instead of $f(x)$ and ϕ individually, since $f(x)$ and ϕ can be separated by the normalized distribution constraint

$$\int \phi f(x) dx = \phi \quad (4)$$

Methods: Inversion Algorithms for Recovery of PSD

B-spline of approximation

In our algorithm, the unknown function $p(x)$ is approximated by a linear combination of B-spline base functions, $B_j^m(x)$, with coefficients c_j which are given by

$$p(x) = \sum_{j=1}^{N} c_j B_j^m(x) + \epsilon(x) \quad (5)$$

Here, $\epsilon(x)$ is the approximation error, and m, N, are the order and dimension of the B-spline, respectively. Unlike piecewise polynomial (PP) representation of spline functions, the B-form representation of spline has the advantages in that the nonlinear PP-form spline functions (such as parabolic and cubic spline) can be described as a linear combination of B-spline basis functions (third- and fourth-order B-spline), as well as linear spline function (second-order B-spline). Thus, a variety of basis spline expansions can be formulated as a linear problem due to the use of B-spline as the unifying basis function (De Boor, 1978). Since B-spline can accurately approximate any smooth function, the use of B-spline functions reduces the number of independent variables to be determined and stabilizes the inversion process.

Using the B-spline approximation, Eq. 2 can be written as

$$\mu_s'(\lambda_i) = \sum_{j=1}^{N} c_j \int K_i(x, \lambda_i) B_j^m(x) dx + E_i \qquad i = 1, \ldots, M \quad (6)$$

where E_i is the summation of measurement error and model (approximation) error.

In matrix notation, Eq. 6 is given by

$$\boldsymbol{b} = \boldsymbol{A}\boldsymbol{f} + \boldsymbol{E} \quad (7)$$

where $\boldsymbol{b}$ is the measurement data and $b_i = \mu_s'(\lambda_i)$; $\boldsymbol{f}$ is unknown function and $f_j = c_j$; $\boldsymbol{E}$ is error; and $\boldsymbol{A}$ is the response model, whose components are

$$a_{i,j} = \int K_i(x, \lambda_i) B_j^m(x) dx \quad (8)$$

In general, the solution to Eq. 7 can be formulated as a classical least-squares problem

$$\min\left\{ \| \boldsymbol{A}\boldsymbol{f} - \boldsymbol{b} \|_2^2 \right\} \quad (9)$$

However, since direct solution of Eq. 9 can yield an unstable solution when measurement data is contaminated with noise, regularization is necessary for reducing the influence of the noise in the inversion process.

Tikhonov regularization

In order to stabilize the inverse solution, we employ Tikhonov regularization in which the regularized solution $\boldsymbol{f}_\alpha$ is defined as the solution of the following optimizing problem:

$$\min\left\{ \| \boldsymbol{A}\boldsymbol{f} - \boldsymbol{b} \|_2^2 + \alpha^2 \| \boldsymbol{L}\boldsymbol{f} \|_2^2 \right\} \quad (10)$$

Here, $\boldsymbol{L}$ is an appropriately chosen regularization matrix. The regularization parameter α controls the weight given to minimization of the regularization term $\| \boldsymbol{L}\boldsymbol{f}_{\text{reg}} \|_2$ relative to minimization of the resident term $\| \boldsymbol{A}\boldsymbol{f}_{\text{reg}} - \boldsymbol{b} \|_2$.

Different ways to choose the regularization matrix $\boldsymbol{L}$ result in different regularization methods, such as zeroth-, first-, and second-order, and entropy regularization (Press et al., 1992). In our algorithm, the second-order regularization form is chosen since it provides the smoothness of the solution, which is often called smoothing constraint

$$\| \boldsymbol{L}\boldsymbol{f}_{\text{reg}} \|_2^2 = \sum_{j=3}^{N} \left(f_j - 2f_{j-1} + f_{j-2} \right)^2 \quad (11)$$

However, the smoothing constraint alone cannot guarantee stable, non-negative solution of size distribution. To avoid a negative solution, the non-negativity constraint should be included

$$p(x) = \sum_{j=1}^{N} f_j B_j^m(x) \geq 0 \quad (12)$$

Equations 10, 11 and 12 constitute the inverse problem in which coefficient f of the B-spline expansion need to be determined. From Eq. 4, the PSD and volume fraction are subsequently obtained. If the regularization parameter α is known, the inverse problem is a linear least-squares problem with linear inequality. In this work, the active-set quadratic programming (QP) method (Gill et al., 1984) was used to solve the PSD inverse problem. The success of this regularization method depends on the choice of optimal regularization parameter α.

Regularization parameter selection

The choice of optimal regularization parameter is important to solve the ill-posed inversion problem. On the one hand, if the parameter is too small, the noise cannot be filtered out and spurious oscillations in the solution exist. On the other hand, if the parameter is too large, some data, as well as noise, are filtered out and the solution is oversmoothed.

Several approaches have been proposed for selecting an appropriate regularization parameter. If the reliable information about error norm $\| \boldsymbol{E} \|_2$ (including model and experiment errors) is available, the discrepancy principle (Morozov, 1984) can be used to choose regularization parameters such that the residual norm for the regularized solution equates the error norm. Ramachandran et al. (1996b) used this approach to recover aerosol-size distribution from cascade impactor data. However, this technique clearly depends on the ability to correctly estimate errors in the measurement data.

Generalized cross validation (GCV) (Wahba, 1977; Golub et al., 1979) is a popular method for choosing the regularization parameter since it does not require an estimation of the error norm. The GCV method is based on statistical considerations that a good regularization parameter can predict missing data values. Elicabe and Garcia-Rubio (1990) used this approach for recovery of polystyrene latex PSD from turbidity measurements. However, GCV cannot be expected to perform well in the case where there are relatively few measurements (Wahba, 1990), and the GCV function may have flat minimum. Consequently, it may be difficult to locate the value of global minimum (Hansen and O'Leary, 1993).

L-curve method (Hansen, 1992) is another parameter choosing method which is independent of error estimates. The L-curve is a plot of regularization term $\| \boldsymbol{L}\boldsymbol{f}_{\text{reg}} \|_2$ vs. residual term $\| \boldsymbol{A}\boldsymbol{f}_{\text{reg}} - \boldsymbol{b} \|_2$ for all regularization parameters. As shown in Figure 1, optimal solution lies near the corner of the "L-curve" since the solution strikes a balance between the solution smoothness and the residual error in this region. Lloyd et al. (1997) used the L-curve method for inversion of PSD from diffusion battery data, and showed that the solution obtained is as good as or better than that obtained by the discrepancy principle or Twomey's method.

In most applications, L-curve method is used for regularization methods which employ a smoothing constraint only. In this article, the L-curve method is used to choose the regularization parameter for the PSD inversion problem contained by both smoothness and non-negativity constraints. A similar approach has been used for recovering PSD from multispectral optical depth measurements (Liu et al., 1999).

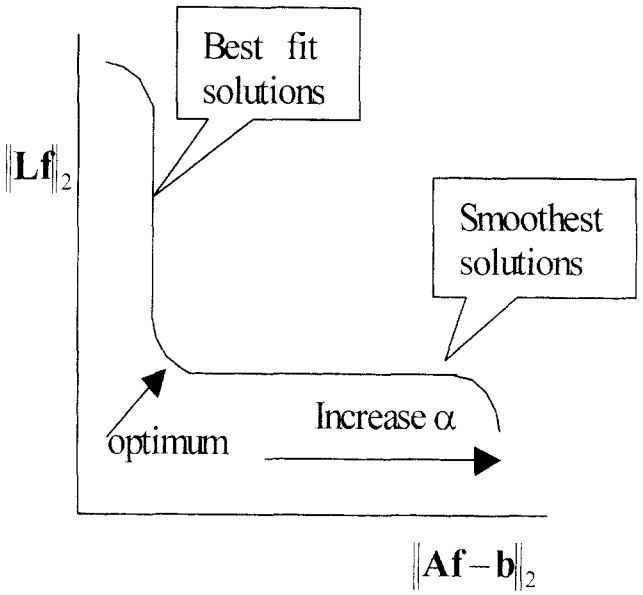

Figure 1. L-curve showing the trade-off between the smoothest solutions and best fit solutions.

In order to investigate the performance of this inversion algorithm, numerical simulations have been made for different types of distributions (that is, unimodal and bimodal, normal and lognormal, narrow and broad). The synthetic data of isotropic scattering coefficients at different wavelengths were calculated from Eq. 1 using an assumed PSD and volume fraction. Ten wavelengths, ranging from 300 nm to 900 nm, were used in the simulation. It is assumed that particles are spherical and the particle-size range of suspensions was from 10 nm to 1,000 nm, so that Mie scattering theory is suitable for scattering calculation. To simulate real experimental conditions, a specific amount of Gaussian random noise was added to the noise-free synthetic data. For convenience, the assumed and recovered size distributions were normalized to a maximum value of one for the purposes of comparison. Following assessment of algorithm performance with synthetic measurements, the algorithm was employed with actual FDPM measurements of titanium dioxide suspensions.

Results and Discussion of Synthetic Studies

The performance of an inverse algorithm depends upon (1) the degree of the error associated with the B-spline approximation; (2) whether measurement error is tolerated; and finally (3) its flexibility to recover various types of size distributions (that is, log-normal, bi-modal, and so on). In order to assess whether both smoothness and non-negativity constraints provide a good solution with respect to other approaches, a comparison of different inversion approaches is also presented.

Effects of model errors

To study the effects of model errors caused by B-spline approximation, we assumed that measurement errors are zero in the synthetic data sets. The assumed "true" distribution is

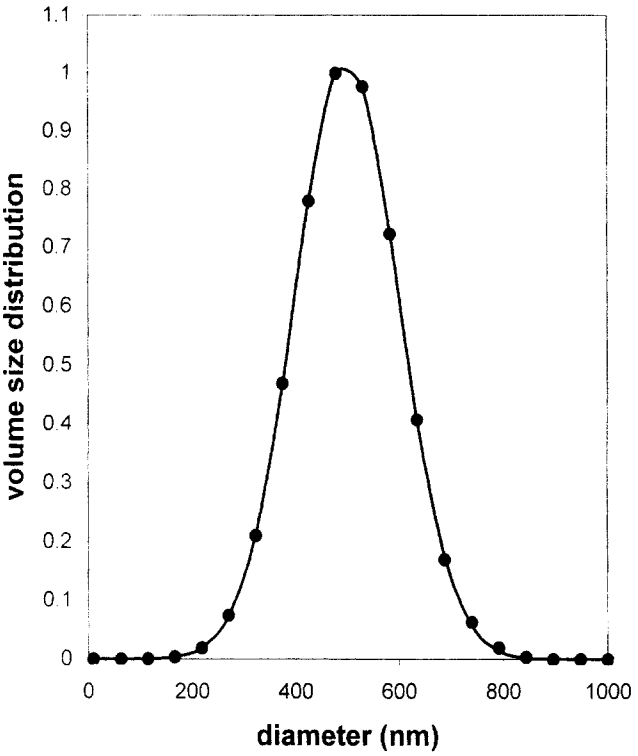

Figure 2. Recovered normal size distribution (symbols) reconstructed from B-spline approximation using noise-free synthetic data and actual size distribution (line) for a normal distribution of colloids with refractive index of titanium dioxide.

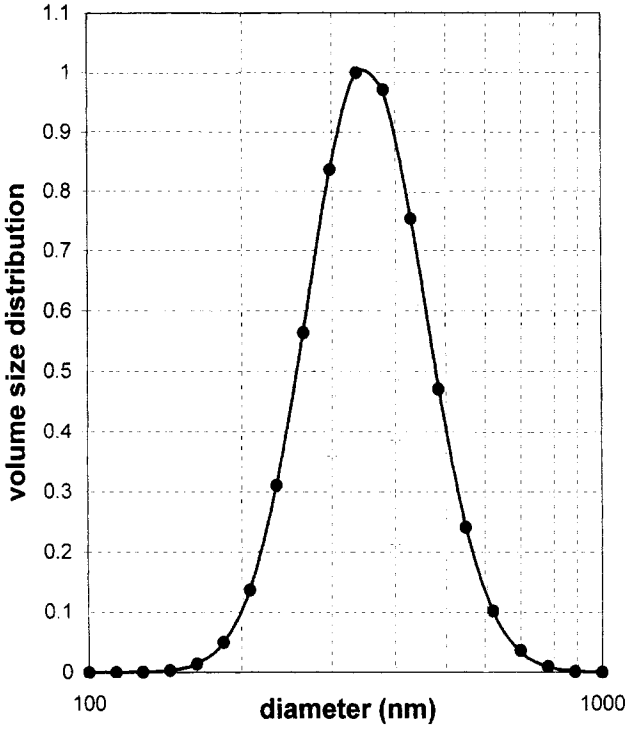

Figure 3. Recovered log-normal size distribution (symbols) reconstructed from B-spline approximation using noise-free synthetic data and actual size distribution (line) for a log-normal distribution of colloids with refractive index of titanium dioxide.

shown as a solid line in Figure 2 for a unimodal Gaussian distribution, and the discrete points denote recovered size distributions approximated by B-spline expansion. The recovered volume fraction, mean size, and standard deviation of size distribution, and corresponding assumed true values are compared in Table 1. Similarly, the assumed "true" and recovered distributions are shown in Figure 3 for log-normal size distribution. For recovery of log-normal distribution, a geometric size scale was used, and the geometric mean size and standard deviation of PSD are obtained and compared to assumed true values, which are shown in Table 2. In these simulations, the regularization parameters selected by L-curve method are very small (2.83×10^{-5} for normal size distribution, and 1.60×10^{-4} for lognormal size distribution), and the recovered solutions were found to match the "true" values well.

From this simulation, we can see that: (1) the B-spline expansions provide a good approximation of size distributions; (2) the inversion algorithm can accurately recover the PSD and volume fraction if there is no measurement error; and (3) the effects of model errors can be neglected, reducing the need for regularization significantly.

Effects of measurement errors

To investigate the effects of measurement errors on our inverse algorithm, we added different levels of random Gaussian noise to the noise-free synthetic measurements. For a unimodal Gaussian-size distribution of titanium dioxide suspension, different noise levels were tested. The inversion results of PSD for three noise levels (1%, 5%, and 10%) are shown in Figure 4. The recovered volume fraction, mean size and standard deviation, and assumed values are also shown in Table 3. A similar simulation was performed using a geometric size scale for recovery of log-normal size distribution and volume fraction, and the results are shown in Figure 5 and Table 4. It can be seen that our inverse algorithm can effectively suppress noise propagation, and provide reason-

Table 1. Effects of Model Errors for Inversion of Unimodal Gaussian Distribution

	Vol. Fraction	Mean Size (nm)	Dev. (nm)
True values	0.01	500	100
Recovered value	0.010003	500.28	100.54

Table 2. Effect of Model Errors for Inversion of Unimodal Log-Normal Distribution

	Vol. Fraction	Geometric Mean (nm)	Geometric Dev.
True values	0.02	350	1.3
Recovered value	0.019997	350.04	1.3006

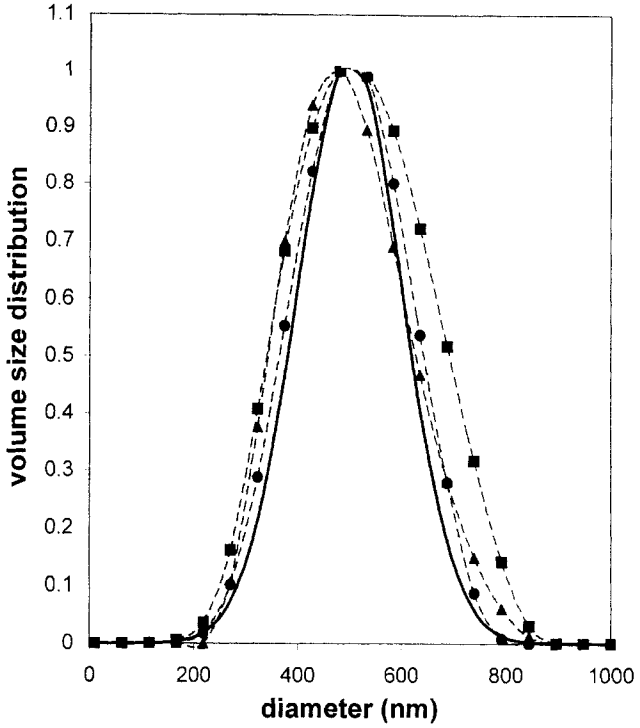

Figure 4. Effects of measurement errors for recovery of unimodal Gaussian distribution.

Recovered-size distributions (symbols) are reconstructed from synthetic data containing 1% (filled circles), 5% (filled triangles), and 10% (filled squares) random noise. The solid line denotes the "true" size distribution.

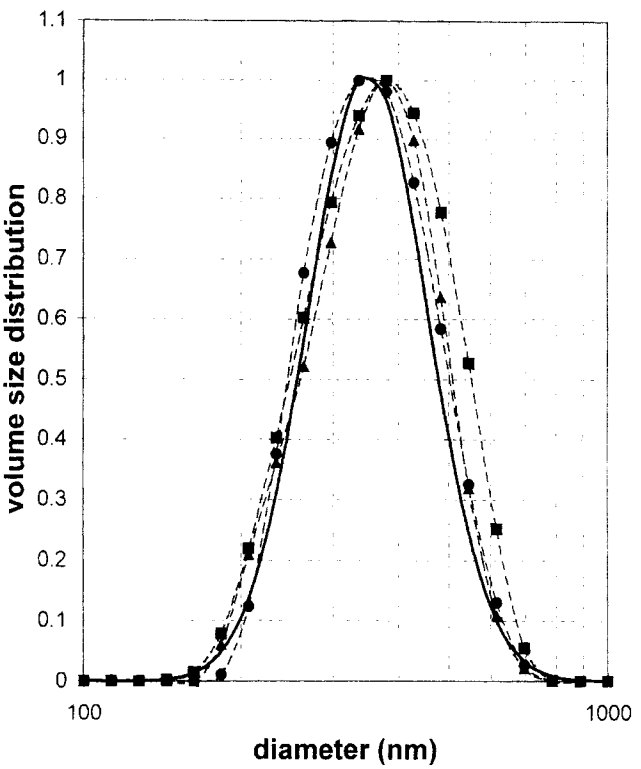

Figure 5. Effects of measurement errors for recovery of unimodal log-normal distribution.

Recovered-size distributions (symbols) are reconstructed from synthetic data containing 1% (filled circles), 5% (filled triangles), and 10% (filled squares) random noise. The solid line denotes the "true" size distribution.

able inversion results for normal and log-normal distributions within as high as 10% measurement error in isotropic scattering coefficients. As the noise level increases, the size distributions are over-smoothed, which may be due to L-curve method. The oversmoothness phenomena by using L-curve method have been reported by Hansen (1998). Although the accuracy of recovered size distributions decreases as the noise level increases, the recovered volume fractions are accurate, and the moments of recovered PSD (that is, mean size and standard deviation) are close to the true values.

In the simulations above, the fourth-order B-spline (cubic spline) was used for approximating the unknown function. Other B-spline basis functions, second and third B-spline (linear and parabolic spline), were also tested for model errors, and different measurement error levels. Similar results were obtained using these different basis functions. Since the inversion results using linear and parabolic B-spline approximation are not as good as those by cubic B-spline approximation at high noise levels, we employ the cubic B-spline approximation in our subsequent work.

Table 3. Effects of Measurement Errors for Inversion of Unimodal Gaussian Distribution

	Vol. Fraction	Mean Size (nm)	Dev. (nm)
True values	0.01	500	100
+1% noise	0.00999	502.67	105.9
+5% noise	0.00979	498.16	113.87
+10% noise	0.01026	519.75	127.53

Inversion methods comparison

From our solutions using synthesis measurements, we found that both the smooth and non-negativity constraints are important for PSD inversion from FDPM measurements. The original Tikhonov regularization method does not include the non-negativity constraints. When used in our problem, it produces unrealistic negative solutions, especially at the limits of particle-size distribution. Similar unrealistic negative solutions have also been reported in the literature (Steele and Turco, 1997; Popovici et al., 1999). Bashurova et al. (1991) suggested replacing the negative values with zero if solution has negative values, but this might not be the best choice in some cases. Figures 6 and 7 show two examples of the comparison of our algorithm with the original Tikhonov method and Bashurova's method for recovery of PSD in titanium dioxide samples, in which the 3% and 8% random Gaussian

Table 4. Effects of Measurement Errors for Inversion of Unimodal Log-Normal Distribution

	Vol. Fraction	Geometric Mean (nm)	Geometric Dev.
True values	0.02	350	1.3
+1% noise	0.02005	352.41	1.305
+5% noise	0.02013	355.22	1.310
+10% noise	0.02030	363.84	1.341

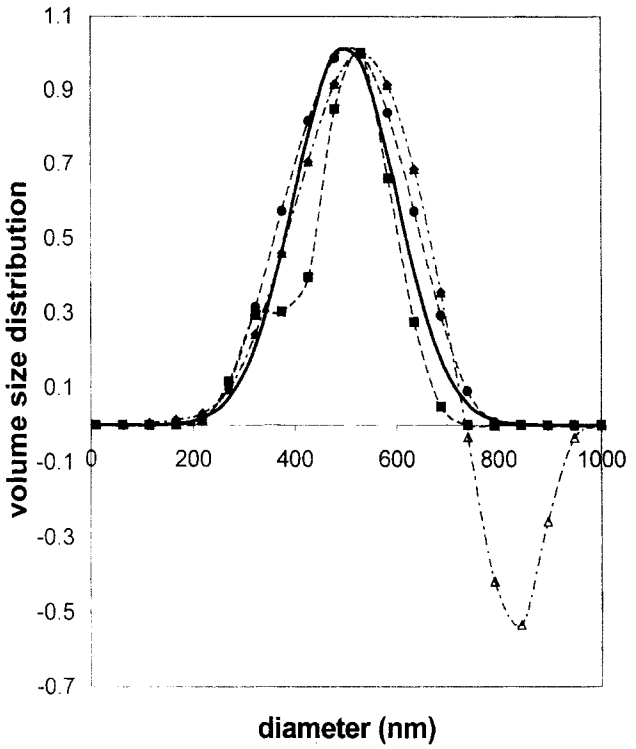

Figure 6. Recovered-size distributions (symbols) reconstructed by our algorithm (filled circles), Tikhonov method (open triangles), Bashurova's method (filled diamonds), and NNLS (filled squares) from synthetic data containing 3% random noise.

The solid line denotes the "true" size distribution.

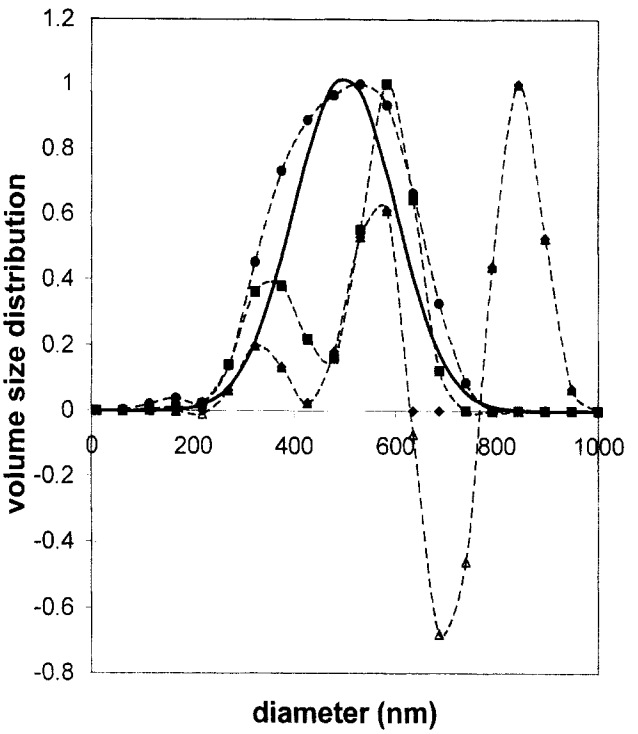

Figure 7. Recovered-size distributions (symbols) reconstructed by our algorithm (filled circles), Tikhonov method (open triangles), Bashurova's method (filled diamonds) and NNLS (filled squares) from synthetic data containing 8% random noise.

The solid line denotes the "true" size distribution.

noise levels were added to simulated data. In each method, L-curve method was used for choosing regularization parameters. The recovered volume fraction, mean size, and standard deviation of size distribution at two different noise levels are shown in Tables 5 and 6, respectively. At the low noise level, the Bashurova's method can overcome the shortcoming of original Tikhonov method, and can achieve a reasonable solution. However, the inversion results are still unsatisfactory when compared to those obtained from our algorithm. This is especially true for recovery of volume fraction. Since the volume fraction is calculated by integrating Eq. 4, directly replacing the negative values with zero values leads to large errors on integration. At high noise levels, both Tikhonov and Bashurova's methods fail to obtain the stable solutions. In contrast, our algorithm obtains reasonable inversion results.

Moreover, the non-negativity constraint alone is not sufficient to give a good solution, especially at large noise levels. We compared our algorithm with the nonnegative least square (NNLS) method (Larson and Hansen, 1974) using the same synthetic data as above, and the results are also shown in Figures 6 and 7, and Tables 5 and 6. Although the recovered volume fraction, mean size, and standard deviation are close to true values, oscillation in the recovered PSD by the NNLS method at the large noise case indicates the need of the smoothness constraint.

Table 5. Various Inversion Results for a Gaussian Distribution with 3% Measurement Noise Added

	Vol. Fraction	Mean size (nm)	Dev. (nm)
True values	0.01	500	100
Our algorithm	0.0102	503.41	107.10
Original Tikhonov method	0.0088	410.82	Not recovered
Bashurova's method	0.0130	510.47	105.90
NNLS method	0.0098	491.29	94.92

Recovery of broad and narrow-size distribution

To further test our algorithm, the quality of reconstruction of narrow and broad size distributions was investigated. Two Gaussian size distributions with the same mean sizes, but dif-

Table 6. Various Inversion Results for a Gaussian Distribution with 8% Measurement Noise Added

	Vol. Fraction	Mean Size (nm)	Dev. (nm)
True values	0.01	500	100
Our algorithm	0.0096	502.67	105.9
Original Tikhonov method	0.0131	680.21	228.25
Bashurova's method	0.0193	686.58	190.48
NNLS method	0.0099	509.60	121.35

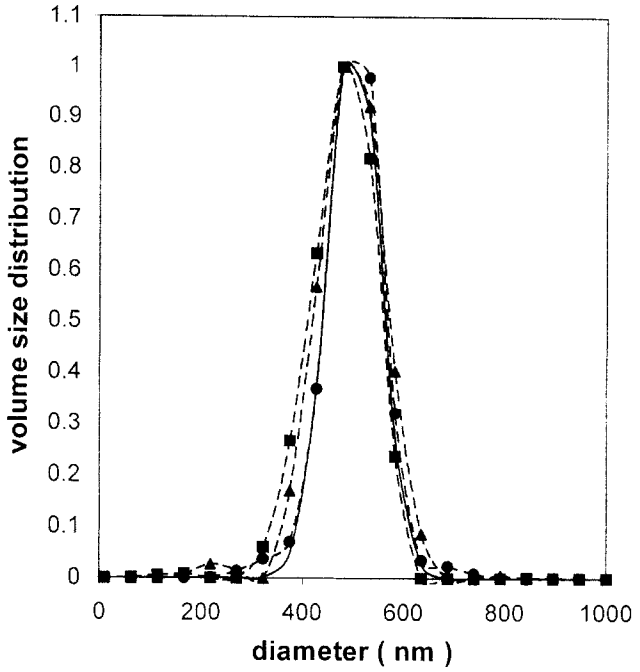

Figure 8. Effects of measurement error for recovery of narrow Gaussian distribution.

Recovered-size distributions (symbols) are reconstructed from synthetic data containing 1% (filled circles), 5% (filled traingles), and 10% (filled squares) random noise. The solid line denotes the "true" size distribution.

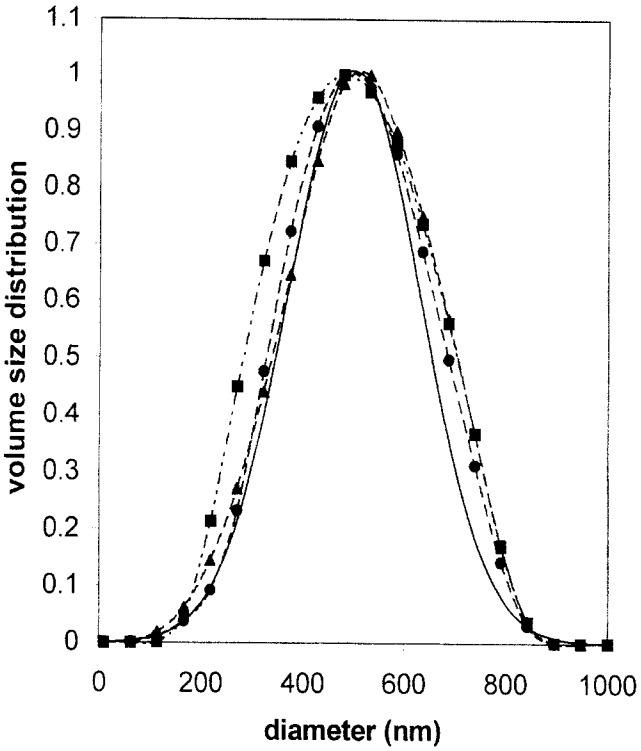

Figure 9. Effects of measurement error for recovery of broad Gaussian distribution.

Recovered size distributions (symbols) are reconstructed from synthetic data containing 1% (filled circles), 5% (filled triangles) and 10% (filled squares) random noise. The solid line denotes the "true" size distribution.

ferent standard deviations, were investigated using synthetic measurements. The recovered PSD at different noise levels (1%, 5% and 10%) are shown in Figures 8 and 9, and the recovered volume fraction, mean size, and standard deviation are listed in Tables 7 and 8. As noise increases, the recovered PSD for the broad distribution are over-smoothed when compared to that for the narrow distribution. However, the relative errors of recovered deviation of broad distribution are smaller than that of narrow distribution, which may be due to the numerical round-off error. From these results, it is found that the effects of polydispersity on the quality of inversion are small, and our algorithm can recover both narrow and broad distributions at different noise levels.

Recovery of the multi-modal-size distribution

Besides unimodal size distributions, the ability of our algorithm to recover bimodal size distribution was also tested numerically. Figure 10 gives the recovered PSD from an assumed bimodal Gaussian distribution, in which no random noise was added to simulated data. Like the unimodal-size distribution, the regularization parameter chosen by L-curve method is very small (5.05×10^{-6}), and the recovered results are in good agreement with assumed true values for bimodal-size distribution. Clearly, it shows that the model errors are negligible, and our algorithm can be successfully used for recovery of bimodal distribution. Furthermore our results demonstrate that the arbitrary assumption of PSD form in *a priori* can be avoided.

The effects of measurement errors were also studied for bimodal-size distribution, which are shown on Figure 11. At a low noise level (within 5%), the first mode shows good agreement with the true value, while the second mode is far away from the true value. Compared to the inversion of unimodal normal distribution, the effects of noise are larger for recovery of bimodal normal distribution, which means that recovery of multi-modal distribution is more sensitive to measurement error than recovery of unimodal distribution. Hence, more accurate and more numerous measurement data are required in order to recover multi-modal size distribution. Al-

Table 7. Effects of Measurement Errors for Inversion of a Narrow Gaussian Distribution

	Vol. Fraction	Mean Size (nm)	Dev. (nm)
True values	0.01	500	50
+1% noise	0.00998	500.55	61.30
+5% noise	0.00988	493.24	70.06
+10% noise	0.00930	476.83	65.45

Table 8. Effects of Measurement Errors for Inversion of a Broad Gaussian Distribution

	Vol. Fraction	Mean Size (nm)	Dev. (nm)
True values	0.01	500	130
+1% noise	0.0101	507.96	135.32
+5% noise	0.0102	512.61	141.77
+10% noise	0.0094	495.57	145.11

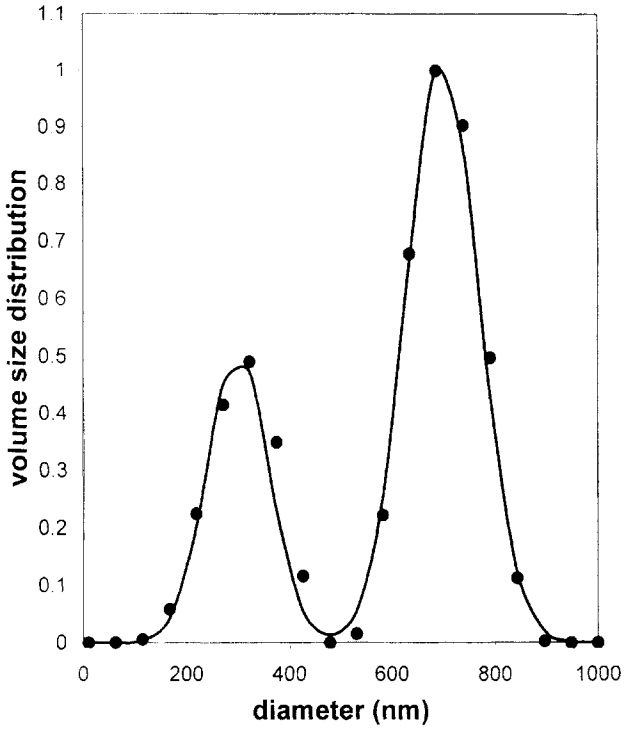

Figure 10. Recovered size distribution (symbols) reconstructed from B-spline approximation using noise-free synthetic data and actual size distribution (line) for a bimodal Gaussian distribution of colloids with refractive index of titanium dioxide.

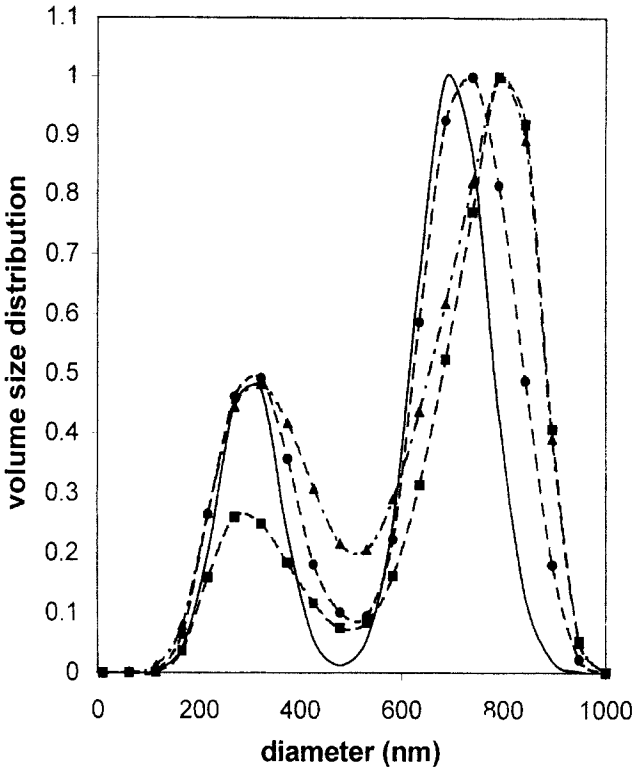

Figure 11. Effects of measurement error for recovery of bimodal Gaussian distribution.

Recovered-size distributions (symbols) are reconstructed from synthetic data containing 1% (filled circles), 5% (filled triangles) and 10% (filled squares) random noise. The solid line denotes the "true" size distribution.

though agreement between retrieved PSD and assumed PSD decreases as noise level increases, the two modes of distribution can be successfully reconstructed within as high as a 10% random measurement error.

Results and Discussion of Experimental Studies

Besides the synthetic study, our algorithm was also tested for recovery of PSD and volume fraction from actual FDPM measurements of titanium dioxide suspensions. Two different samples of titanium dioxide suspensions with different size distributions were kindly provided by Dupont, and FDPM measurements were performed by Richter (2000). The volume fractions are 0.04 in both samples measured by evaporation experiments, which are high enough to be in the multiple scattering regime, but low enough to prevent interparticle interactions. In our previous inversion work, the log-normal distribution was assumed, and nonlinear optimization methods were subsequently used to obtain the parameters of assumed distributions from measured isotropic scattering coefficients. However, using our current approach, no *a priori* information of size distribution is needed, and the inversion process is more computationally efficient.

The recovered size distributions of two samples using our algorithm are shown in Figures 12 and 13, respectively. For comparison, recovered PSD from FDPM measurements of some samples using assumption of log-normal form of distribution, and measured PSD from dynamic light scattering (DLS) measurement at dilute samples (Richter, 2000) are also shown in Figures 12 and 13. For sample A, the size distribution derived from X-ray sedimentation measurement was provided by Dupont, which is also shown in Figure 12. In our algorithm, a geometric size scale was used for recovery of size distributions, and a comparison of geometric mean size, standard deviation of size distribution, and volume fraction by different approaches are presented in Tables 9 and 10. For sample A, the particle-size distributions recovered by different approaches are close even though they may not match very well. The recovered geometric mean size and standard deviation by our algorithm are comparable with previous inversion results, DLS, and X-ray measurements, and the recovered volume fractions are accurate when compared to evaporation measurements. The difference between inversion results may be due to measurement errors in the different approaches. For sample B, from Figure 13 and Table 10, we can see that the size distribution recovered by free form inversion is closer to DLS results than that recovered using the assumption of log-normal form of distribution, even though the assumption of log-normal form was also used in DLS measurements. Compared to the evaporation experiment, volume fraction of suspensions can always be accurately obtained by our algorithm.

For sample B, other inverse methods, the original Tikhonov regularization, Bashurova's method, and NNLS were also used

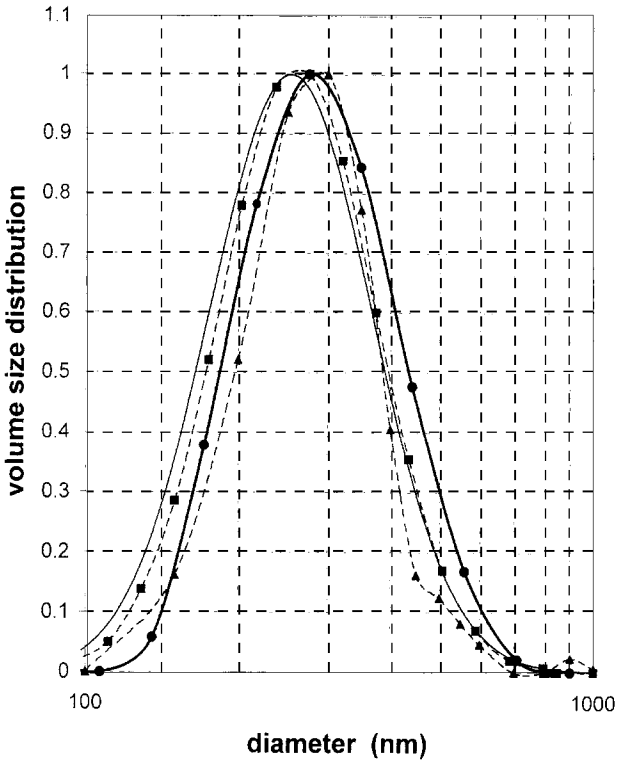

Figure 12. Comparison of recovered PSD by free-form inversion (solid line with filled circles) with log-normal form inversion (solid line), DLS (dashed line with filled squares) and X-ray (dashed line with filled triangles) measurements of titanium dioxide sample A.

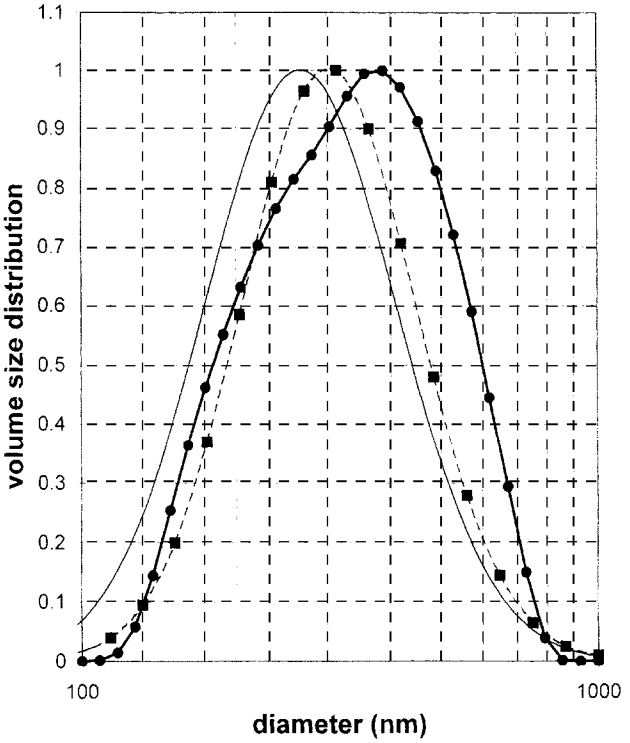

Figure 13. Comparison of recovered PSD by free-form inversion (solid line with filled circles) with log-normal form inversion (solid line) and DLS results (dashed line with filled squares) of titanium dioxide sample B.

for comparison, and results are shown in Figure 14 and Table 11. We can see that the PSD recovered by NNLS method oscillates even though the recovered geometric mean size and standard deviation are closer to DLS results. Although, in this case, the negative value problem is avoided so that Bashurova's method gives the same solution as Tikhonov regularization, the difference between the inversion results from the Tikhonov regularization and the DLS results is larger than that between the inversion results from our algorithm results and the DLS results.

Summary and Conclusion

A new inverse algorithm was proposed for recovery of free form PSD and volume fractions from FDPM measurements in opaque colloidal suspensions. In this method, the size distribution was approximated by B-spline approximation. Tikhonov regularization along with both non-negativity and smoothing constraints, in which L-curve method was used to choose the regularization parameter, was used to ensure the stable and realistic solution. The simulation results show that both constraints are very important for recovery of PSD. Furthermore, the inversion of measurement data to obtain PSD is over-smoothed as the noise increases, which may be due to the L-curve method to choose regularization parameters.

Our algorithm can be used for recovery of many different types of particle-size distributions, including normal and log-normal, narrow and broad, and unimodal and multimodal distributions. The inversion results from synthetic data show that this algorithm is insensitive to model error, and has a high stability in the presence of measurement errors. Within 5% noise in synthetic measurements, our inverse algorithm can effectively suppress noise propagation, and provide good

Table 9. Various Particle Sizing Results for Actual Experimental Data on Titanium Dioxide Sample A

	Vol. Fraction	Geometric mean (nm)	Geometric Dev.
DLS results	Not available	262.25	1.414
X-ray results	Not available	270.81	1.358
Log normal inversion	0.00394	253.30	1.444
Free form inversion	0.00391	284.56	1.431

Table 10. Various Particle Sizing Results for Actual Experimental Data on Titanium Dioxide Sample B

	Vol. Fraction	Geometric Mean (nm)	Geometric Dev.
DLS measurement	Not available	303.11	1.467
Lognormal inversion	0.00389	265.66	1.530
Free form inversion	0.00398	327.28	1.504

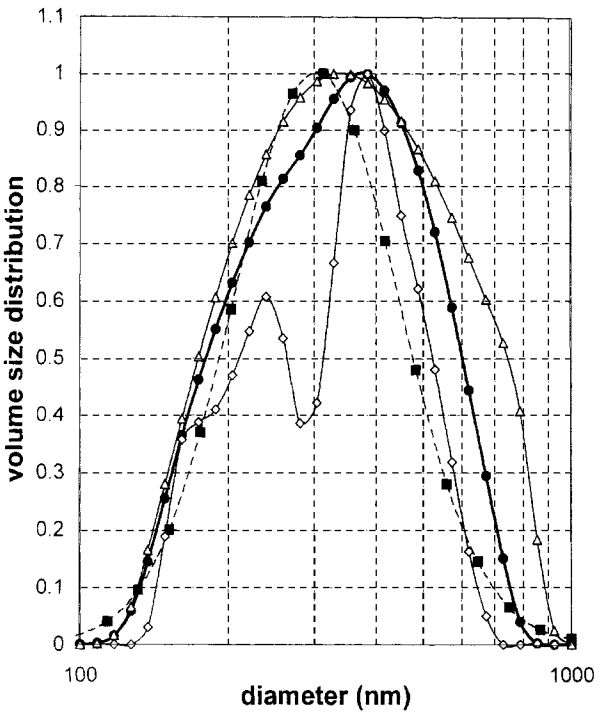

Figure 14. Recovered size distributions (symbols) by our algorithm (solid line with filled circles), Tikhonov method (solid line with open triangles), and NNLS (solid line with open diamonds) from actual FDPM measurement of titanium dioxide sample B.

The dashed line with filled squares denotes the PSD recovered from DLS measurements.

inversion results. Compared to recovery of unimodal-size distribution, it is more sensitive to measurement error for recovery of multimodal distribution. Further work will focus on how to improve the accuracy and precision of FDPM measurements in order to recover multimodal size distribution from real FDPM experimental data.

Our algorithm was also tested by recovery of unimodal size distributions from actual experimental data of FDPM measurements. The recovered size distributions and their moments (that is, mean size and deviation) by our algorithm are comparable with previous inversion results, DLS, and X-ray measurements. The recovered volume fractions are accurate compared with evaporation experiments. Compared to our previous inversion method, this method avoids the arbitrary assumption of *a priori* PSD forms. Also, our current linear inverse method is faster than the previous nonlinear inverse method, and is more suitable for *in situ* PSD and volume fraction determination in industry.

Finally, while this algorithm was tested in concentrated, yet noninteracting suspensions, its framework can be modified to include the static structure factor in order to deal with particle interactions. Future work focuses on characterizing interacting suspensions using our algorithm.

Table 11. Various Inversion Results from Actual Experimental Data on Titanium Dioxide Sample B

	Vol. Fraction	Geometric Mean (nm)	Geometric Dev.
DLS measurement	Not available	303.11	1.467
Our Algorithm	0.00398	327.28	1.504
Tikhonov method	0.00420	348.73	1.577
NNLS method	0.00391	320.08	1.458

Acknowledgment

This work is supported in parts by the National Science Foundation (CTS-9876583), The Dow Chemical Company, and the DuPont Young Faculty Fellow Program. The authors acknowledge Stewart Wood and Mohsen Khalili for their guidance and suggestion.

Notation

a_1 = size lower limit
a_2 = size upper limit
A = matrix (response model)
b = measurement data
B = B-spline function
c = coefficients of B-spline
D = diffusion coefficient
e = measurement error
E = error matrix
f = unknown function matrix
$f(x)$ = particle-size distribution
g = scattering anisotropy
K = kernel function
m = order of B-spline
M = number of experiment data
n = refraction index
N = dimension of B-spline
p = unknown function
Q_{scat} = scattering efficiency
q = isotropic source
r = position
t = time
U = total photon density
v = speed of light
x = particle diameter
α = regularization
$\bullet$ = model error
λ = wavelength
μ_a = absorption coefficient
μ_s' = isotropic scattering coefficient
ϕ = volume fraction

Literature Cited

Aalto, P., U. Tapper, P. Paatero, and T. Raunemaa, "Deconvolution of Particle-Size Distributions by Means of Extreme Value Estimation Method," *J. Aerosol Sci.*, **21**, S159 (1990).

Alba, F., G. M. Crawley, J. Fatkin, D. M. J. Higgs, and P. G. Kippax, "Acoustic Spectroscopy as a Technique for the Particle Sizing of HIgh Concentration Colloids, Emulsions and Suspensions," *Colloid Surf. A*, **153**, 495 (1999).

Amato, U., and W. Hughes, "Maximum-Entropy Regularization of Fredholm Inegral-Equations of the 1st Kind," *Inverse Probl.*, **7**, 793 (1991).

Amato, U., D. DiBello, F. Esposito, C. Serio, G. Pavese, and F. Romano, "Intercomparing the Twomey Method with a Multimodal Lognormal Approach to Retrieve the Aerosol Size Distribution," *J. Geophys. Res.-Atmos.*, **101**, 19267 (1996).

Bashurova, V. S., K. P. Koutzenogil, A. Y. Pusep, and N. V. Shokhirev, "Determination of Atmospheric Aerosol Size Distribution—Function From Screen Diffusion Battery Data—Mathematical Aspects," *J. Aerosol Sci.*, **22**, 373 (1991).

Bohren, C., and D. Huffmann, *Absorption and Scattering of Light by Small Particles*, Wiley, New York (1983).
Carfora, M. F., F. Esposito, and C. Serio, "Numerical Methods for Retrieving Aerosol Size Distributions from Optical Measurements of Solar Radiation," *J. Aerosol Sci.*, **29**, 1225 (1998).
Chahine, M. T., "Determination of the Temperature Profile in an Atmosphere from its Outgoing Radiance," *J. Opt. Soc. Amer.*, **58**, 1634 (1968).
Copper, D. W., and L. A. Spielman, "Data Inversion Using Nonlinear Programming with Physical Constraints: Aerosol Size Distribution Measurement by Impactors," *Atmos. Environ.*, **10**, 723 (1976).
Crawley, G., M. Cournil, and D. DiBenedetto, "Size Analysis of Fine Particle Suspensions by Spectral Turbidimetry: Potential and Limits," *Powder Technol.*, **91**, 197 (1997).
De Boor, C., *A Practical Guide to Splines*, Springer, New York (1978).
Duderstadt, J. J., and L. J. Hamilton, *Nuclear Reactor Analysis*, Wiley, New York (1976).
Elicabe, G. E., and L. H. Garcia-Rubio, "Latex Particle-Size Distribution From Turbidimetric Measurements—Combining Regularization and Generalized Cross-Validation Techniques," *Adv. Chem. Ser.*, 83 (1990).
Ferri, F., A. Bassini, and E. Paganini, "Modified Version of the Chahine Algorithm to Invert Spectral Extinction Data for Particle Sizing," *Appl. Opt.*, **34**, 5829 (1995).
Fishkin, J. B., P. T. C. So, A. E. Cerussi, S. Fantini, M. A. Franceschini, and E. Gratton, "Frequency-Domain Method for Measuring Spectral Properties in Multiple-Scattering Media—Methemoglobin Absorption-Spectrum in a Tissuelike Phantom," *Appl. Opt.*, **34**, 1143 (1995).
Frock, H. N., "Particle-Size Determination Using Angular Light-Scattering," *ACS Sym Ser.*, **332**, 146 (1987).
Frontini, G., and J. Chaubell, "Inversion of Turbidity Measurements of Polymer Latex Using Wavelet Functions," *Chemometrics Intell. Lab. Syst.*, **47**, 89 (1999).
Gill, P. E., W. Murray, M. A. Saunders, and M. H. Wright, "Procedures for Optimization Problems with a Mixture of Bounds and General Linear Constraints," *ACM Trans. Math. Softw.*, **10**, 282 (1984).
Golub, G. H., M. Heath, and G. Wahba, "Generalized Cross Validation as a Method for Choosing a Good Ridge Parameter," *Technometrics*, **21**, 215 (1979).
Hansen, P. C., "Relations Between SVD and GSVD of Discrete Regularization Problems in Standard and General-Form," *Linear Alg. Appl.*, **141**, 165 (1990).
Hansen, P. C., "Numerical Tools for Analysis and Solution of Fredholm Integral-Equations of the First Kind," *Inverse Probl.*, **8**, 849 (1992).
Hansen, P. C., and D. P. O'Leary, "The Use of the L-Curve in the Regularization of Discrete Ill-Posed Problems," *SIAM J. Sci. Comput.*, **14**, 1487 (1993).
Hansen, P. C., *Rank-Deficient and Discrete Ill-Posed Problems: Numerical Aspects of Linear Inversion*, SIAM, Philadelphia (1998).
Hopke, P. K., and P. Paatero, "Extreme-Value Estimation Applied to Aerosol-Size Distributions and Related Environmental-Problems," *J. Res. Natl. Inst. Stand. Technol.*, **99**, 361 (1994).
Horne, D. S., and C. M. Davidson, "Application of Diffusing-Wave Spectroscopy to Particle Sizing in Concentrated Dispersions," *Colloid Surf. A*, **77**, 1 (1993).
Ishimaru, A., *Wave Propagation and Scattering in Random Media*, Academic Press, San Diego (1978).
Larson, C. L., and R. J. Hanson, *Solving Least Squares Problems*, Prentice-Hall, Englewood Cliffs, NJ (1974).
Lehner, D., G. Kellner, H. Schnablegger, and O. Glatter, "Static Light Scattering on Dense Colloidal Systems: New Instrumentation and Experimental Results," *J. Colloid Interface Sci.*, **201**, 34 (1998).
Ligon, D. A., T. W. Chen, and J. B. Gillespie, "Determination of Aerosol Parameters from Light Scattering Data Using an Inverse Monte Carlo Technique," *Appl. Opt.*, **35**, 4297 (1996).
Liu, Y. G., W. P. Arnott, and J. Hallett, "Particle Size Distribution Retrieval from Multispectral Optical Depth: Influences of Particle Nonsphericity and Refractive Index," *J. Geophys. Res.-Atmos.*, **104**, 31753 (1999).
Lloyd, J. J., C. J. Taylor, R. S. Lawson, and R. A. Shields, "The Use of the L-Curve Method in the Inversion of Diffusion Battery Data," *J. Aerosol Sci.*, **28**, 1251 (1997).
Markowski, G. R., "Improving Twomey Algorithm for Inversion of Aerosol Measurement Data," *Aerosol Sci. Technol.*, **7**, 127 (1987).
Morozov, V. A., *Methods for Solving Incorrectly Posed Problems*, Springer, New York (1984).
Nascimento, C. A. O., R. Guardani, and M. Giulietti, "Use of Neural Networks in the Analysis of Particle Size Distributions by Laser Diffraction," *Powder Technol.*, **90**, 89 (1997).
Nicoli, D. F., T. Kourti, P. Gossen, J. S. Wu, Y. J. Chang, and J. F. Macgregor, "Online Latex Particle-Size Determination By Dynamic Light-Scattering—Design for an Industrial-Environment," *ACS Sym. Ser.*, **472**, 86 (1991).
Popovici, M. A., N. Mincu, and A. Popovici, "A Comparative Study of Processing Simulated and Experimental Data in Elastic Laser Light Scattering," *Math. Biosci.*, **157**, 321 (1999).
Press, W., S. Teukolsky, W. Vetterling, and B. Flannery, *Numerical Recipes in FORTRAN: The Art of Scientific Computing*, Cambridge University Press, New York (1992).
Ramachandran, G., and M. Kandlikar, "Bayesian Analysis for Inversion of Aerosol Size Distribution Data," *J. Aerosol Sci.*, **27**, 1099 (1996a).
Ramachandran, G., E. W. Johnson, and J. H. Vincent, "Inversion Techniques for Personal Cascade Impactor Data," *J. Aerosol Sci.*, **27**, 1083 (1996b).
Richter, S. M., R. R. Shinde, G. V. Balgi, and E. M. Sevick-Muraca, "Particle Sizing Using Frequency Domain Photon Migration," *Part. Part. Syst. Charact.*, **15**, 9 (1998).
Richter, S. M., and E. M. Sevick-Muraca, "Characterization of Concentrated Colloidal Suspensions Using Time-Dependent Photon Migration Measurements," *Colloid Surf. A*, **172**, 163 (2000).
Richter, S. M., "Frequency Domain Photon Migration for the Characterization of Concentrated Particulate Suspensions," PhD Diss. Purdue University (2000).
Shinde, R., G. Balgi, S. Richter, S. Banerjee, J. Reynolds, J. Pierce, and E. Sevick-Muraca, "Investigation of Static Structure Factor in Dense Suspensions by Use of Multiply Scattered Light," *Appl. Opt.*, **38**, 197 (1999).
Sevick-Muraca, E., J. Pierce, H. B. Jiang, and J. Kao, "Photon-Migration Measurement of Latex Size Distribution in Concentrated Suspensions," *AIChE J.*, **43**, 655 (1997).
Steele, H. M., and R. P. Turco, "Retrieval of Aerosol Size Distributions from Satellite Extinction Spectra Using Constrained Linear Inversion," *J. Geophys. Res.-Atmos.*, **102**, 16737 (1997).
Thomas, J. C., "Fiber Optic Dynamic Light-Scattering From Concentrated Dispersions—Potential for Online Particle-Size Measurement," *ACS Symp. Ser.*, **472**, 98 (1991).
Tikhonov, A. N., and V. Y. Arsenin, *Solutions of Ill-Posed Problems*, Wiley, New York (1977).
Twomey, S., "Comparison of Constrained Linear Inversion and an Iterative Nonlinear Algorithm Applied to the Indirect Estimation of Particle Size Distributions," *J. Comput. Phys.*, **18**, 188 (1975).
Wahba, G., "Practical Approximate Solutions to Linear Operators Equations When the Data are Noisy," *SIAM J. Numer. Anal.*, **14**, 651 (1977).
Wahba, G., *Spline Models for Observation Data*, SIAM, Philadelphia, PA (1990).
Xu, P. L., "Truncated SVD Methods for Discrete Linear Ill-Posed Problems," *Geophys. J. Int.*, **135**, 505 (1998).
Ye, M., S. M. Wang, Y. Lu, T. Hu, Z. Zhu, and Y. Q. Xu, "Inversion of Particle Size Distribution from Angular Light Scattering Data with Genetic Algorithms," *Appl. Opt.*, **38**, 2677 (1999).

Manuscript received June 20, 2000, and revision received Dec. 19, 2000.